

63-3-3

AFCRL-63-285

403135



THE PENNSYLVANIA
STATE UNIVERSITY

IONOSPHERIC RESEARCH

Scientific Report No. 180

THEORETICAL DETERMINATION OF THE IMPEDANCE CHARACTERISTICS OF A CAPACITIVE IONOSPHERE ROCKET PROBE

by

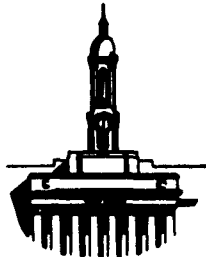
J. R. Herman

March 1, 1963

"The research reported in this document has been sponsored by the Geophysics Research Directorate of the Air Force Cambridge Research Laboratory, Office of Aerospace Research, United States Air Force, under Contract AF19(604)-8012."

"This research sponsored by Defense Atomic Support Agency, Washington, D. C. under Web No. 07.077."

IONOSPHERE RESEARCH LABORATORY



403135
CATALOGUED BY ASTIA
AS AD NO.

University Park, Pennsylvania

Contract No. AF19(604)-8012
Project 7663, Task 766301

AFCLR - 63-285

IONOSPHERIC RESEARCH

Contract AF19(604)-8012

Scientific Report

on

"Theoretical Determination of the Impedance
Characteristics of a Capacitive Ionosphere Rocket Probe"

by

J. R. Herman

March 1, 1963

Scientific Report No. 180

(Project 7663, Task 766301)

Ionosphere Research Laboratory

"The research reported in this document has been sponsored by the Geophysics Research Directorate of the Air Force Cambridge Research Laboratories, Office of Aerospace Research, United States Air Force, under Contract AF19(604)-8012."

"This research sponsored by Defense Atomic Support Agency, Washington, D.C. under Web No. 07.007."

Submitted by:

John S. Nisbet (aw)
J. S. Nisbet, Assistant Professor of
Electrical Engineering, Project Supervisor

Approved by:

A. H. Waynick
A. H. Waynick, Professor of Electrical
Engineering, Director, IRL

The Pennsylvania State University
College of Engineering
Department of Electrical Engineering

TABLE OF CONTENTS

Abstract	1
1. INTRODUCTION	1
2. GENERAL STATEMENT OF THE PROBLEM	4
3. QUALITATIVE FEATURES OF THE THEORETICAL MODEL	6
4. THEORETICAL CONSIDERATIONS AND DISCUSSION	9
4.1 ION CURRENTS	12
4.2 ELECTRON CURRENTS	21
4.3 THE COMPLEX IMPEDANCE COMPONENTS	26
4.4 THE APPLICATION OF MAGNETOIONIC THEORY	27
4.5 TWO DIMENSIONAL APPROXIMATION	37
4.6 THREE DIMENSIONAL APPROACH	49
4.7 EQUIVALENT CIRCUIT REPRESENTATION	52
5. NUMERICAL EVALUATION OF THE THEORETICAL RESULTS	56
6. CONCLUSION	66
6.1 SUGGESTIONS FOR FURTHER RESEARCH	68
ACKNOWLEDGEMENTS	69
BIBLIOGRAPHY	70

ABSTRACT

The impedance characteristics of a capacitive ionospheric rocket probe have been determined as a function of the electron density, collision frequency, and temperature. The physical model used in developing the theory incorporated both effects of the ion sheath which forms about the rocket body and the anisotropic nature of the surrounding magneto-ionic medium. Results are obtained and numerically evaluated to show that the sheath makes a very significant contribution to the impedance characteristics.

1. INTRODUCTION

The general characteristics of the ionospheric electron density profile below 120 km have been determined by several methods using instruments carried by rockets. These methods are of great interest since ground based radio techniques have not lead to reliable determinations of the electron density profile below 120 km. In 1950 some data were obtained, between 30 and 80 km, by the use of rocket borne Gerdien capacitors at White Sands, New Mexico, giving one of the first estimates of the conductivity of this region. Bourdeau, Whipple, and Clark (1959) analysed the Gerdien capacitor data based on the assumptions that cosmic radiation is the principle source of ionisation at lower altitudes, and that the contribution of free electrons to the negative conductivity is negligible below 80 km. The results appeared to indicate that the effect of the shock front surrounding the rocket on the conductivity was not significant.

Since about 1957, a great deal of work has been done towards developing a reliable rocket probe applicable to the lower portions of the ionosphere. Some of the more popular methods are radio frequency impedance probes for measuring the electron density, Langmuir probes for electron temperature, electron density, or ion density, Gerdien capacitors as mentioned above, and combinations of these and other methods employed simultaneously to utilize the

best features of each.

The RF probe technique for the determination of ionospheric parameters uses the impedance characteristics of a probe immersed in a plasma. In flights of RF probes discussed by Jackson and Pickar (1957), the ionosphere was observed to have an effect on the impedance of a rocket borne antenna operated at high frequencies. This effect was later used as the basis of an electron density probe by Kane, Jackson, and Whale (1962). They obtained an electron density profile which agrees in form with the profile reduced from ionosonde data above 120 km. In this paper an attempt was made to account for the sheath effects by considering the sheath to be an empirically determined cylindrical capacitor which was assumed to be concentric with the antenna. The anisotropy of the ionosphere was also considered. However Kane, Jackson, and Whale's analysis is only applicable where the collision frequency is low compared to the collision frequency in the 50 to 120 km region.

An analysis of a rocket probe experiment, which seems more suitable for the 50 to 120 km region of the ionosphere, was made by R. F. Mlodnosky and O. K. Garriott (1962). In this experiment a small low frequency RF voltage was impressed upon a capacitor built into the nose of a rocket. When the rocket passed through the ionosphere, the impedance of the capacitor changed in response to the

changes in the electron density, collision frequency, and temperature. The frequency of the voltage was high enough so that the ions present were unable to follow the voltage changes, and far enough below the plasma frequency so that the electron motion was in phase with the applied voltage. Their analysis assumed that the capacitive coupling between the sheath and the rocket would be the dominant factor in determining the impedance characteristics of the probe. The presentation given by Miodnosky and Garriott demonstrated the feasibility of this type of rocket probe.

The Langmuir probe technique (Langmuir, 1931) is based upon the Boltzmann equation for ionized gases. When an electrode is placed in a plasma, such as the ionosphere, and the current to it is measured as a function of the potential applied to the electrode, the resulting current-voltage curves permit the evaluation of the electron temperature and density. Rocket flights using a Langmuir probe have been employed a great deal since 1949. Some of the people engaged in the early Langmuir probe measurements were G. Hok (1951), E. O. Johnson (1950), and J. C. Seddon (1953). However it was not until recently that the theory of such probes as applied to the ionosphere has begun to be developed. A paper by L. G. Smith (1961) discusses the qualitative features of this theory quite thoroughly. He points out that the method is limited by the sweep rate of the programmed potential, and that the

theory fails to account for the earth's magnetic field or for the ion sheath that forms about the rocket. A similar experiment, discussed by Hoegy and Brace (1961), using a dumbbell shaped probe, accounted for the sheath and the magnetic field in the theory. However, here too the results are good only above 120 km, and even in this region there remain some large discrepancies in the measured temperature to be explained. The Langmuir probe theory, while well developed for laboratory measurements, is still far from being a well developed theory when applied to the ionosphere. In particular, the Langmuir probe analysis does not apply to the lower altitudes.

2. THE GENERAL STATEMENT OF THE PROBLEM

A rocket probe flight similar to the one described by Mlodnosky and Garriott is planned for the near future by the Ionosphere Research Laboratory of the Pennsylvania State University. The main purpose of this experiment will be to measure the electron density as a function of altitude between 50 and 120 km. A low frequency RF probe was selected because of its ability to single out electrons while rejecting ion and dust particles on the basis of their respective masses. Therefore, it is desirable that a theoretical investigation of the probe be conducted to aid in the interpretation of the experimental data.

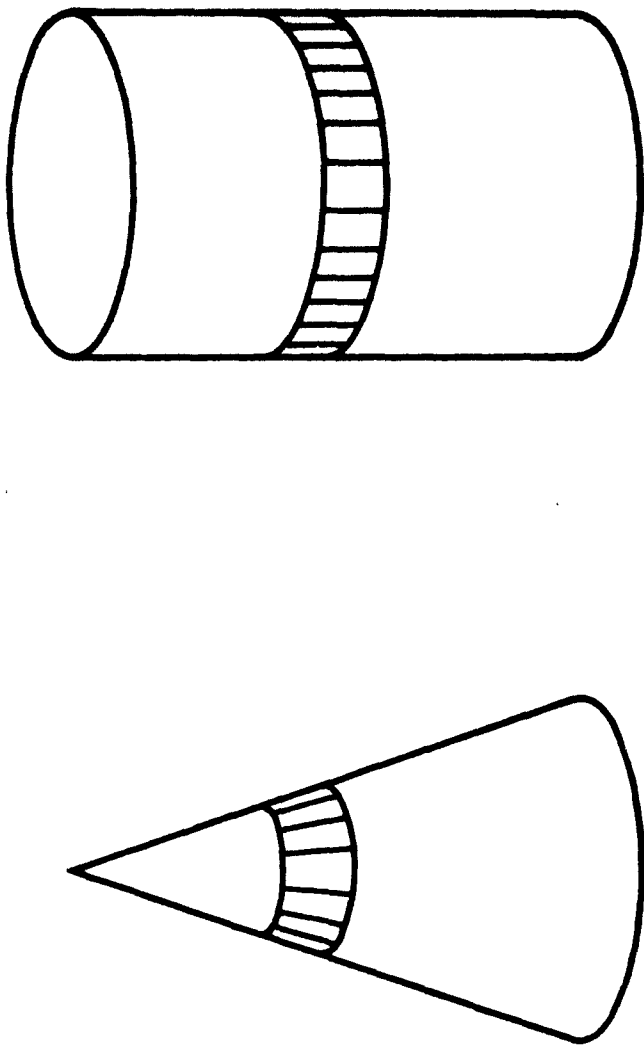
The specific problem to be considered will be

the investigation of the contributions to the impedance characteristics of a low frequency RF capacitor probe immersed in the ionosphere as a function of altitude, and to find the relationship between the measured probe impedance and the electron density.

3. QUALITATIVE FEATURES OF THE THEORETICAL MODEL

The capacitor probe is built into the conical nose of a rocket by splitting the cone into two sections separated by a dielectric slab. This split cone is connected by a wire to each of its two metallic portions to a source of low frequency RF voltage. Unfortunately, the conical geometry is extremely difficult to analyse so that a similarly split cylinder was considered instead; Fig.1. The substitution of a cylinder for a cone will be shown to have little effect on the results. From the application of a low frequency RF voltage to the capacitor, we wish to determine its complex impedance in a slowly changing, inhomogeneous, conducting, and anisotropic medium. Finally, the electron density will be related to the measured impedance.

If an undisturbed body is placed in a neutral plasma composed of negative electrons and positive ions, such as the ionosphere, then both ions and electrons will contribute to a current from the plasma to the body. In the ionosphere the electron mean thermal velocity is always much greater than the corresponding ion velocity. This results in a net accumulation of negative charge on the body. The accumulating negative charge reduces the electron flow until the electron and ion currents are equal. This constitutes the equilibrium condition. Thus,



MODEL OF ROCKET NOSE AND THE CYLINDRICAL APPROXIMATION

FIGURE 1

a region of space will surround the body which has a deficiency of electrons relative to a neutral plasma. Such a region is known as an ion sheath as it contains a net positive charge attributable to the positive ions. The thickness of the sheath depends on the electron and ion temperatures and concentrations as well as on the velocity of the body through the ionosphere.

Since the definition of capacitance is based on the ratio of the charge stored within the capacitor to the voltage impressed upon it, the region between the edge of the body and the edge of the sheath clearly makes a contribution to the capacitance of the body. This capacitance will change as the parameters describing the ionosphere change. Another contribution to the capacitance, in the case of the split cylinder, is the capacitance between the two halves separated by a dielectric insulator. Here again the characteristics of the medium surrounding the capacitor are intimately connected with the value of the measured capacitance. The combined contributions of these effects will yield the impedance and capacitance as a function of the electron density, temperature, and collision frequency.

4. THEORETICAL CONSIDERATIONS AND DISCUSSION

The theoretical discussion will be divided into several distinct steps. First, an estimate of the sheath thickness will be obtained on the basis of a simple model. From this estimated thickness and a consideration of the velocity distribution of the ions and electrons in the ionosphere, the currents to the split cylinder will be obtained. These currents will in turn permit a computation of the capacitance and the conductivity associated with the sheath. Second, a computation of the capacitance and the conductivity associated with the oscillation of the electronic charge between the two halves of the cylindrical capacitor will be made. This computation will take into account the effects of the anisotropic nature of the ionosphere based on a tensor description.

An estimate of the sheath thickness may be made from a model based on the work of Hoegy and Brace (1961) and Jastrow and Pearse (1957). Assume we have a cylinder immersed in a plasma about which an ion sheath has formed. At a distance r_0 from the center of the cylinder the net charge density is assumed to fall to zero. In the actual case the net charge density falls to zero smoothly but rapidly as the distance from the center increases. However, it will be assumed that a sharp boundary exists for the purposes of the calculation. The positive charge

contained within the sheath exactly cancels the negative charge q on the cylinder. Then, if V_0 is the potential on the cylinder, it will be related to the charge q by

$$\frac{1}{R} \frac{\partial}{\partial R} \left(R \frac{\partial V}{\partial R} \right) = - \frac{Ne}{\epsilon_0}, \quad (1)$$

with the boundary conditions

$$V = 0 \quad \text{when } R \geq r_0,$$

$$V = V_0 \quad \text{when } R = r.$$

Then the expression for the potential inside the sheath is given by

$$V = - \frac{Ne}{4\epsilon_0} R^2 + B \ln R + C, \quad (2)$$

where

$$B = \frac{1}{\ln r_0/r} \left[\frac{Ne}{4\epsilon_0} (r_0^2 - r^2) - V_0 \right],$$

$$C = \frac{Ne}{4\epsilon_0} r_0^2 - B \ln r_0.$$

The charge q is given by $q = - \pi h N e (r_0^2 - r^2)$,

and

h = the height of the cylinder in meters,

N = the quantity of charge per cubic meter,

- r_0 = the sheath radius in meters,
 r = the cylinder radius in meters,
 e = 1.60206×10^{-19} coulombs,
 V = the potential in volts,
 V_0 = the potential at the cylinder surface.

The preceding calculation can be used to estimate part of the capacitance and conductance G (in amperes per volt) of the cylindrical capacitor in the ionosphere (Mlodnosky and Garriott, 1962). As long as the plasma frequency is greater than the oscillator frequency, the application of a small sinusoidal voltage will cause a current to flow in phase with the applied voltage. Then we may write

$$G = \frac{\Delta I}{\Delta V} ,$$

where ΔI and ΔV are measured internally at the generator. The value $dV = \Delta V/2$ is measured across the sheath so that

$$G = \frac{1}{2} \frac{dI}{dV} .$$

The amount of charge variation arising from changes in the sheath dimension with the applied voltage gives rise to a component of current in phase quadrature with the applied voltage. This current accounts for a capacitive reactive part of the admittance G , and is given by

$$C = \frac{1}{2} \frac{dq}{dv} ,$$

or more usefully,

$$C = \frac{1}{2} \left(\frac{dq/dR}{dv/dR} \right) \Big|_{v = v_0} . \quad (3)$$

Similarly for G,

$$G = 1/2 \left(\frac{dI/dR}{dv/dR} \right) \Big|_{v = v_0} . \quad (4)$$

In order to use equations (3) and (4) it will be necessary to enter into a calculation of the currents which flow from the ionosphere to the cylinder. The computation of the ion and electron currents will be carried out separately.

It will be assumed that outside of the sheath the presence of the cylinder is not felt in the ionosphere.

4.1 ION CURRENTS

Since the rocket velocity will normally be much greater than the ion thermal velocity, the main contribution to the ion current will result from the interception of the ions by the speeding rocket. In addition, the ion mass is so large that the ions are unable to respond to the voltage changes on the order of 100 kc. This means

that the ion current from the ionosphere to the rocket is virtually independent of the rocket's potential with respect to the ionosphere.

Assume that all the ions which intercept the sheath boundary are collected at the cylindrical conducting surface. If a surface element dS is moving with a velocity u_x along the x axis, and the following quantities are defined,

n = the unit normal vector to dS ,

k = Boltzmann's constant (1.38×10^{-23} joules/ $^{\circ}K$),

v = the particle velocity in meters per second,

T = the temperature in degrees Kelvin,

m = the particle mass in kilograms,

j = the current density in amperes/square meter,

u = the rocket velocity in meters per second,

then the number of particles per unit volume with velocities between v and $v + dv$ is

$$dN = \frac{N}{a_1^3 \pi^{3/2}} \exp(-v^2 a_1^2) dv \quad (5)$$

$$a_1^{-1} = \sqrt{2kT/m_1} \quad \text{and}$$

$$v^2 = v_x^2 + v_y^2 + v_z^2 .$$

The subscript 1 will denote the ions and 2 the electrons.

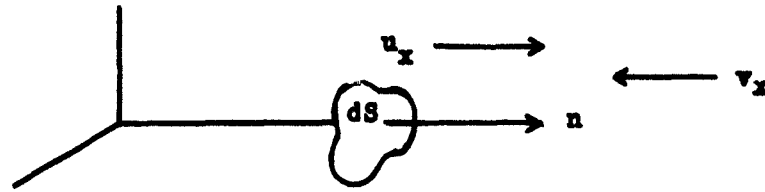


Figure 2

The current density j_x is then

$$j_x = \int e (v_x + u_x) dN. \quad (6)$$

The limits of integration are given by

$$\begin{aligned} 0 &\leq v_x + u_x < \infty, \\ -\infty &\leq v_y < \infty, \\ -\infty &\leq v_z < \infty. \end{aligned}$$

The following standard integrals will be used.

$$\int_{-\infty}^{\infty} e^{-a^2 v^2} dv = \frac{1}{a} \sqrt{\pi}. \quad (7a)$$

$$\int_{-\infty}^{\infty} v_x e^{-a^2 v_x^2} dv_x = \frac{1}{2} \frac{e^{-a^2 v_x^2}}{a^2}. \quad (7b)$$

$$u \int_{-\infty}^{\infty} e^{-a^2 v^2} dv = \frac{\sqrt{\pi}}{2a} u (1 + \operatorname{erf} u a), \quad (7c)$$

where

$$\operatorname{erf} u = \frac{2}{\sqrt{\pi}} \int_0^u e^{-v^2} dv.$$

Using the definition for a_1 , we have

$$j_x = \frac{Ne}{2\sqrt{\pi} a_1} \left[\sqrt{\pi} a_1 u_x (1 + \operatorname{erf} a_1 u_x) + e^{-a_1^2 u_x^2} \right] \quad (8a)$$

Equation (8a) is readily generalised. Since n is the unit normal to dS , let u make an angle β with n and write

$$j = \frac{Ne}{2\sqrt{\pi} a_1} \left[\sqrt{\pi} a_1 u \cdot n (1 + \operatorname{erf} a_1 u \cdot n) + e^{-a_1^2 (u \cdot n)^2} \right] \quad (8b)$$

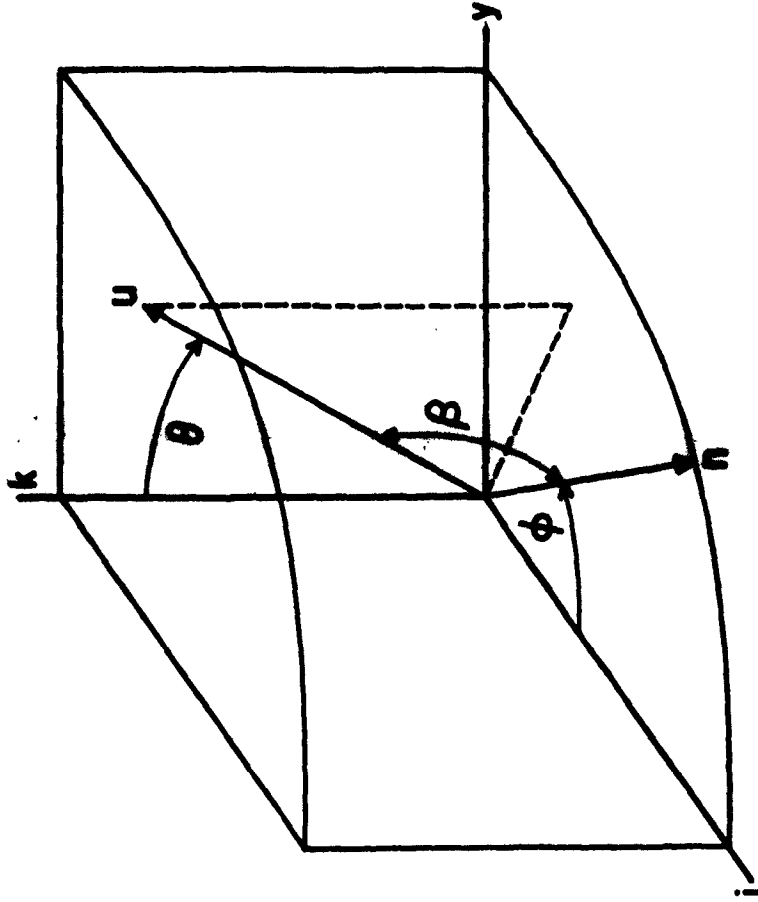
Referring to Figure 3,

$$u \cdot n = u(\underline{u} \cdot \underline{i}) \cos \phi + u(\underline{u} \cdot \underline{j}) \sin \phi,$$

where the quantities \underline{u} , \underline{i} , \underline{j} , and \underline{k} are unit vectors.

Integrating j over the cylindrical surface S yields the total current through that surface. To this we must add the current j_c intercepted by the effective cross sectional area in order to obtain the total ion current to the cylinder. The total ion current I is

$$I = \iint_S j \, dS + \pi r^2 j_c \quad (9a)$$



A CYLINDRICAL SECTION OF THE ROCKET BODY SHOWING THE VELOCITY VECTOR U AND THE SURFACE NORMAL n

FIGURE 3

$$\begin{aligned}
I = & r_0 K \int_0^h \int_0^{2\pi} \left[\sqrt{\pi} A u \cos \phi (1 + \operatorname{erf} A u \cos \phi) \right. \\
& \left. + e^{-A^2 u^2 \cos^2 \phi} \right] d\phi dz + r_0 K \int_0^h \int_0^{2\pi} \left[\sqrt{\pi} B u \sin \phi \right. \\
& \left. (1 + \operatorname{erf} B u \sin \phi) + e^{-B^2 u^2 \sin^2 \phi} \right] d\phi dz \\
& \pi r^2 K \left[\sqrt{\pi} a_1 u \cos \theta (1 + \operatorname{erf} a_1 u \cos \theta) \right. \\
& \left. + e^{-a_1^2 u^2 \cos^2 \theta} \right] , \tag{9b}
\end{aligned}$$

where

$$K = \frac{H e}{\sqrt{\pi} 2 a_1} ,$$

$$A = a_1 (\underline{u} \cdot \underline{i}) ,$$

$$B = a_1 (\underline{u} \cdot \underline{j}) .$$

Since the rocket velocity is very much greater than the mean ion thermal velocity, the cylinder radius is used to estimate the effective cross section rather than the sheath radius. When the sheath radius is very much larger than the rocket radius, the forces within the sheath are far too small to deflect the ions toward the cylinder.

It is now necessary to compute several integrals.

$$I_1 = \int_0^{2\pi} u \cos \phi \, d\phi .$$

$$I_2 = \int_0^{2\pi} Au \cos \phi \operatorname{erf}(Au \cos \phi) \, d\phi .$$

$$I_3 = \int_0^{2\pi} \exp(-A^2 u^2 \cos^2 \phi) \, d\phi .$$

$$I_4 = \int_0^{2\pi} u \sin \phi \, d\phi .$$

$$I_5 = \int_0^{2\pi} Bu \sin \phi \operatorname{erf}(Bu \sin \phi) \, d\phi .$$

$$I_6 = \int_0^{2\pi} \exp(-B^2 u^2 \sin^2 \phi) \, d\phi .$$

It is apparent that $I_1 = I_4 = 0$. I_3 and I_6 may be evaluated by using

$$J_n(z) = \frac{(z/2)^n}{\sqrt{\pi} \Gamma(n + 1/2)} \int_0^\pi e^{iz \cos \phi} \sin^{2n} \phi \, d\phi ,$$

(from Tables of Functions by Jahnke and Emde, 1938), where $J_n(z)$ is a Bessel function. This gives

$$I_3 = 2\pi \exp(-A^2 u^2/2) J_0(1 A^2 u^2/2) , \quad (10)$$

$$I_6 = 2\pi \exp(-B^2 u^2/2) J_0(-i B^2 u^2) \quad (11)$$

Integrating by parts and using a variation of the above form of the Bessel function,

$$J_n(x) = \frac{\exp(-n\pi/2)}{\pi} \int_0^\pi e^{ix \cos \phi} \cos n\phi \, d\phi \quad ,$$

I_2 and I_5 are found to be

$$I_2 = 2\sqrt{\pi} A^2 u^2 e^{-A^2 u^2/2} \left[J_0(i A^2 u^2/2) - i J_1(i A^2 u^2/2) \right] \quad , \quad (12)$$

$$I_5 = 2\sqrt{\pi} B^2 u^2 e^{-B^2 u^2/2} \left[J_0(-i B^2 u^2/2) + i J_1(-i B^2 u^2/2) \right] \quad . \quad (13)$$

Now $I = \iint_S j \, dS + \pi r^2 j_c$ is the total ion current intercepted by the sheath and presumed collected by the cylinder within. Thus,

$$I = K h r_0 \left[\sqrt{\pi} (I_2 + I_5) + I_3 + I_6 \right] + \pi r^2 j_c \quad , \quad (14)$$

or in detail,

$$\begin{aligned}
I = & K r_0 h \left[2\pi A^2 u^2 e^{-A^2 u^2/2} \left[J_0(i A^2 u^2/2) \right. \right. \\
& - i J_1(i A^2 u^2/2) \\
& + 2\pi B^2 u^2 e^{-B^2 u^2/2} \left[J_0(-i B^2 u^2/2) \right. \\
& + i J_1(-i B^2 u^2/2) \\
& + 2\pi \left[e^{-A^2 u^2/2} J_0(i A^2 u^2/2) \right. \\
& \left. \left. + e^{-B^2 u^2/2} J_0(-i B^2 u^2/2) \right] \right] \\
& + K r^2 \left[\sqrt{\pi} a_1 u \cos \theta (1 + \operatorname{erf}(a_1 u \cos \theta)) \right. \\
& \left. + e^{-a_1^2 u^2 \cos^2 \theta} \right].
\end{aligned} \tag{15}$$

When the arguments for the Bessel functions are large and where $u \cdot i$ is taken to be zero, equation (15) becomes

$$\begin{aligned}
I = & 2\sqrt{\pi} K r_0 h \left[2a_1 u \cos \alpha + \frac{1}{a_1 u \cos \alpha} \right] \\
& + \pi r^2 j_0.
\end{aligned} \tag{16}$$

Unfortunately, under ordinary conditions the asymptotic approximation to the Bessel function may not be made.

4.2 ELECTRON CURRENT

The electrons must be considered from another viewpoint. Here both the small mass of the electron and the high mean thermal velocity relative to the rocket suggests that the particle trajectories be examined. From the time an electron enters a region under the rocket's influence to the time when it is either collected or again outside of the region of influence, the rocket may be considered stationary.

In examining the electron particle trajectories within the sheath, we are primarily interested in finding the limiting values of the velocity that will permit the electrons to strike the cylinder surface S . The rocket flight may be roughly broken into two parts. First, a region corresponding to the lower altitudes where the electrons will undergo many collisions before striking the cylinder, and second, where the electrons will be able to traverse the distance between the sheath and the rocket without collisions. In the lower region the contribution of the electron current to the impedance will be overshadowed by the contribution arising from the interelectrode capacitance. Therefore, collisions within the sheath will be neglected for the computation of the electron

current during the entire flight.

Given a cylinder of radius r surrounded by a sheath of radius r_0 , let us assume that an electron intercepts the sheath edge, at A in Figure 4, and attempt to calculate the limiting conditions on its velocity so that it will barely graze the cylinder. Let the velocity be decomposed into a component tangential to the sheath v_θ , a component in the radial direction v_r , and a component in the axial direction v_s . The field between A and B is assumed to be conservative and repulsive with respect to electrons. As stated above, no collisions are assumed to occur while the electrons traverse the path between A and B.

Under these conditions, the minimum value the radial component v_r may have is

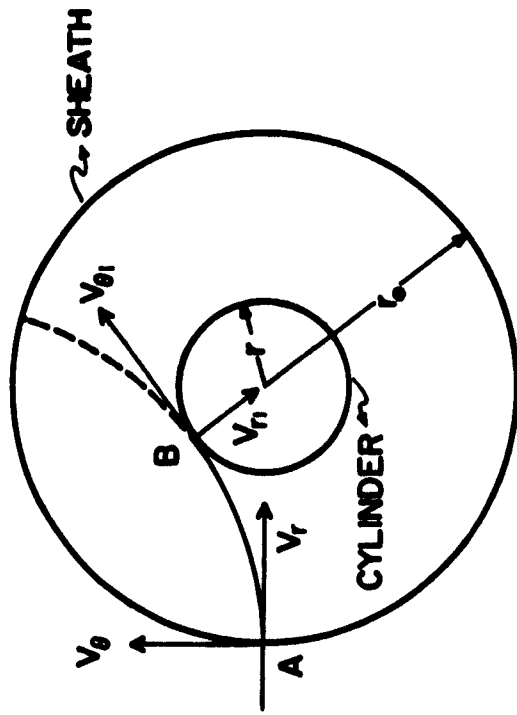
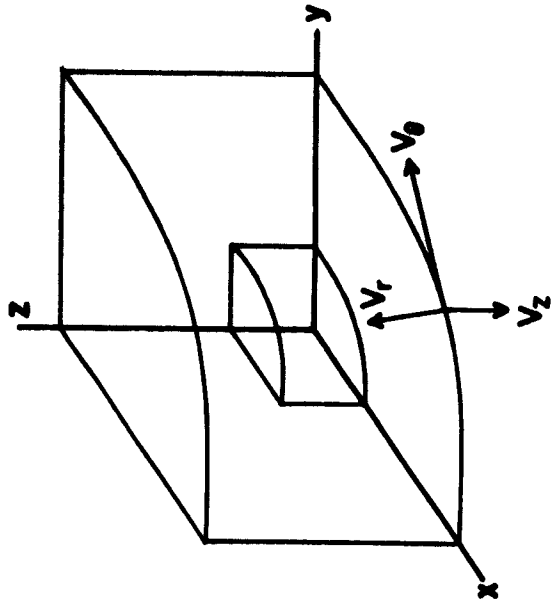
$$v_r = (-2eV_0/m_2)^{1/2} .$$

Conservation of energy and angular momentum requires that

$$\frac{1}{2} m_2 (v_\theta^2 + v_r^2 + v_s^2) = \frac{1}{2} m_2 (v_{\theta 1}^2 + v_{r 1}^2 + v_s^2) - eV_0 ,$$

$$m_2 r_0 v_\theta = m_2 r v_{\theta 1} .$$

$v_{r 1}$ and $v_{\theta 1}$ are the values of the radial and tangential components of the velocity at B. Since $v_{r 1} = 0$ at B,



ELECTRON VELOCITY COMPONENTS

FIGURE 4

$$v_{\theta}^2 \text{ max} = \frac{v_r^2 + \frac{2eV_0}{m_2}}{(r_0/r)^2 - 1},$$

where m_2 = the electron mass in kg (9.11×10^{-31} kg).

The electron current may now be calculated by assuming a Maxwellian distribution of velocities.

Defining $a_2 = (m_2/2kT)^{1/2}$, the electron current i is

$$i = 2\pi r_0 h N_0 \frac{a_2^2}{\pi^{3/2}} \int_{v_z} \int_{v_{\theta}} \int_{v_r} v_r e^{-a_2^2(v_r^2 + v_{\theta}^2 + v_z^2)} dv_r dv_{\theta} dv_z,$$

where the limits of integration are found from

$$\begin{aligned} -\infty \leq v_z \leq \infty, \quad (2eV_0/m_2)^{1/2} \leq v_r \leq \infty, \\ 0 \leq v_{\theta} \leq \sqrt{\frac{v_r^2 + 2eV_0/m_2}{(r_0/r)^2 - 1}}. \end{aligned}$$

The zero limit on v_{θ} arises from the fact that this component of velocity is to be taken as positive regardless of the direction it may assume.

Define $L = 2\pi r_0 h N_0 a_2^3/\pi^{3/2}$, and consider the following integrals:

$$\int_{-\infty}^{\infty} dv e^{-a^2 v^2} = \frac{1}{a} \sqrt{\pi}.$$

$$\int_0^{\infty} v e^{-a_2^2 v^2} dv = \frac{\sqrt{\pi}}{2a_2} \operatorname{erf}(a_2 v_{0z}).$$

Therefore,

$$i = \frac{\pi L}{2a_2^2} \int_0^{\infty} dv_r v_r e^{-a_2^2 v_r^2} \operatorname{erf} \left[a_2 \frac{v_r^2 + \frac{2eV}{M}}{(r_0/r)^2 - 1} \right].$$

After a change of variables we need only consider the integral

$$I_7 = \int_0^{\infty} s e^{-D^2 s^2} \operatorname{erf}(as) ds, \quad D = a \sqrt{(r_0/r)^2 - 1}.$$

Integrating by parts and noting that $(D^2 + a^2)$ is always greater than zero gives

$$i = \frac{\pi L (r_0^2/r^2 - 1)}{8a_2 D^2} \frac{\sqrt{\pi}}{(a^2 + D^2)^{1/2}} e^{-\frac{eV_0}{kT}},$$

or

$$i = \frac{N e \pi r h}{4 a_2} e^{-\frac{eV_0}{kT}} \quad (17)$$

4.3 THE COMPLEX IMPEDANCE COMPONENTS

We have now calculated the expressions for both the electron and ion currents. It must be emphasized that the above analysis applies only when the voltage changes are slow enough so that the electrons fully respond in phase with the voltage. The sheath radius and the potential on the rocket may now be obtained when the rocket is at equilibrium with the ionosphere.

The condition of electrical equilibrium demands that $I = i$. Using this condition and solving for the potential V_0 yields

$$V_0 = \frac{kT}{e} \ln\left(\frac{4a_2}{N_0 e r h} I\right). \quad (18a)$$

Since the derivative of equation (2) is equal to $-q/2\pi r_0 h$, another expression for V_0 is

$$-V_0 = \frac{N_0 e}{4\epsilon_0} \left[r^2 + r_0^2 \left(\ln \frac{r_0^2}{r^2} - 1 \right) \right]. \quad (18b)$$

The elimination of V_0 between these two equations results in a transcendental equation which determines the sheath radius r_0 . This equation is

$$\frac{kT}{e} \ln\left(\frac{N_0 e r h}{4a_2 I}\right) = \frac{N_0 e r^2}{4\epsilon_0} \left[1 + \frac{r_0^2}{r^2} \left(\ln \frac{r_0^2}{r^2} - 1 \right) \right]. \quad (19)$$

Graphical solution of equation (19) on a digital computer permits the use of equations (3) and (4) to obtain the expressions for the capacitance and conductance arising from the ion and electron currents and the sheath fluctuations. These are

$$C = \frac{\pi \epsilon_0 h}{\ln(r_0/r)} \quad , \quad (20)$$

$$G = \frac{1}{2} \left[\left(\frac{kT}{e} \right) i + \frac{I - \pi r^2 j_c}{\frac{N_0}{2\epsilon_0} r^2 \ln(r_0^2/r^2)} \right] \quad . \quad (21)$$

The computation of equations (20) and (21) will be combined with the results of the next section to give the total impedance characteristics of the rocket capacitor probe.

4.4 THE APPLICATION OF MAGNETOIONIC THEORY

The second part of the problem is the calculation of the contribution to the capacitance and the conductance from the electrons oscillating between the two halves of the split cylinder. The approach will be based upon a development of the Appleton-Hartree equations taking into account both the magnetic field of the earth and collisions with neutral particles. The collisions will be expressed through a quantity known as the collision frequency, that is, the effective number of collisions per second.

Consider an electron under the influence of an oscillating electromagnetic field and the earth's magnetic field. The collisions which result from the oscillating motion cause a dissipation of electromagnetic energy in the form of heat and work. It may be shown, Budden (1961), that the forces from the oscillations of the magnetic field are negligible compared to the electric field forces. The peak voltage used will be quite small, so that very little heating due to the applied field will result. This restriction avoids considerations of power loss due to so called acoustic waves, as discussed by Kane, Jackson, and Whale (1962).

First a tensor description of the ionospheric medium will be developed and applied by use of Poynting's theorem to calculate the power dissipated in the medium. Second, an alternate method will be employed, which will turn out to be quite superior to the use of Poynting's theorem. However, it will be shown that both descriptions agree on a qualitative basis. Finally, the various contributions to the capacitance and conductance will be combined in an equivalent circuit which represents the actual rocket probe electrically. The Poynting vector treatment will be seen to be very sensitive to the method of computing the electric field surrounding the rocket and to the geometry used. The second method, based directly on the definition of capacitance, is easily applicable

to any body having cylindrical symmetry.

The differential equation describing the motion of an electron in an anisotropic medium with collisions is

$$m \frac{d^2 r}{dt^2} = qE + q\mu_0 \left(\frac{dr}{dt} \times H \right) - m\nu \frac{dr}{dt}, \quad (22)$$

where

m = the mass of an electron in kg

q = the charge of an electron in coulombs

E = the electric field in volts per meter

μ_0 = permeability of free space in henry's/meter

H = the earth's magnetic field in ampere-turns per meter

ν = the collision frequency of electrons with neutrals

ω = the angular frequency of the oscillator

X' = the electric susceptibility

P = the polarization

σ = the tensor polarisability

N = the electron density per cubic meter

The following basic equations will be used.

$$P = \sigma E, \quad (23a)$$

$$\sigma = \epsilon_0 X' , \quad (23b)$$

$$E = E_0 e^{i\omega t} , \quad (23c)$$

$$P = P_0 e^{i\omega t} , \quad (23d)$$

$$P = N e r . \quad (23e)$$

where r is the displacement of an electron from some reference point designated at time $t = 0$. Equation (22) in component form becomes

$$eE_x = m\ddot{x} - \mu_0 e H_z \dot{y} + \mu_0 e H_y \dot{z} + m v \dot{x}$$

$$eE_y = m\ddot{y} - \mu_0 e H_x \dot{z} + \mu_0 e H_z \dot{x} + m v \dot{y}$$

$$eE_z = m\ddot{z} - \mu_0 e H_y \dot{x} + \mu_0 e H_x \dot{y} + m v \dot{z}$$

By using (23d) and (23e), and the following definitions, the above may be reduced to matrix form.

$$Y = \frac{\mu_0 e}{m\omega} H . \quad (24a)$$

$$X = \frac{Ne^2}{m\omega^2} . \quad (24b)$$

$$Z = \frac{v}{\omega} . \quad (24c)$$

$$\begin{bmatrix} E_x \\ E_y \\ E_s \end{bmatrix} = \begin{bmatrix} -\frac{1}{X} + \frac{iZ}{X} & -i\frac{Y_s}{X} & i\frac{Y_y}{X} \\ i\frac{Y_s}{X} & -\frac{1}{X} + \frac{iZ}{X} & -i\frac{Y_x}{X} \\ -i\frac{Y_y}{X} & i\frac{Y_x}{X} & -\frac{1}{X} + \frac{iZ}{X} \end{bmatrix} \begin{bmatrix} P_x \\ P_y \\ P_s \end{bmatrix} .$$

Therefore, by using (23a) and $U = 1 - iZ$, the inverse of the tensor polarizability is

$$\sigma^{-1} = \begin{bmatrix} -U & -iY_s & iY_y \\ iY_s & -U & -iY_x \\ -iY_y & iY_x & -U \end{bmatrix} \frac{1}{X} .$$

Inverting this matrix yields the tensor polarizability σ

$$= \frac{X}{U(Y^2 - U^2)} \begin{bmatrix} U^2 - Y_x^2 & -iUY_s - Y_x Y_y & iUY_y - Y_x Y_s \\ iUY_s - Y_y Y_x & U^2 - Y_y^2 & -iUY_x - Y_y Y_s \\ -iUY_y - Y_s Y_x & iUY_x - Y_s Y_y & U^2 - Y_s^2 \end{bmatrix} .$$

When H is along the s axis σ becomes,

$$e = X \begin{bmatrix} \frac{U}{Y^2 - U^2} & \frac{-1 Y_s}{Y^2 - U^2} & 0 \\ \frac{1 Y_s}{Y^2 - U^2} & \frac{U}{Y^2 - U^2} & 0 \\ 0 & 0 & \frac{U^2 - Y_s^2}{(Y^2 - U^2)U} \end{bmatrix}$$

Using the fact that $e = e_0 + \sigma$ we have

$$e = \begin{bmatrix} e_0 + \frac{UX}{Y^2 - U^2} & -\frac{1 Y_s X}{Y^2 - U^2} & 0 \\ \frac{1 Y_s X}{Y^2 - U^2} & e_0 + \frac{UX}{Y^2 - U^2} & 0 \\ 0 & 0 & e_0 - \frac{X}{U} \end{bmatrix}$$

Define the following quantities:

$$K_T = e_0 + \frac{UX}{Y^2 - U^2} ,$$

$$K_P = e_0 - \frac{X}{U} ,$$

$$K_H = \frac{Y_s X}{Y^2 - U^2} .$$

Therefore,

$$K_T = \epsilon_0 + \frac{X(1 - iZ)}{Y^2 - (1 - iZ)^2} , \quad (25a)$$

$$K_P = \epsilon_0 - \frac{X}{1 - iZ} , \quad (25b)$$

$$K_H = \frac{Y_2 X}{Y^2 - (1 - iZ)^2} . \quad (25c)$$

Thus, we have

$$\epsilon = \begin{bmatrix} K_T & -i K_H & 0 \\ i K_H & K_T & 0 \\ 0 & 0 & K_P \end{bmatrix} . \quad (26)$$

The matrix form of ϵ in the equation above will be assumed to be a good description of the ionosphere's electrical behavior in the region below 150 km. In other words, we are assuming an anisotropic, inhomogeneous, and dissipative medium that is slightly perturbed by an electromagnetic disturbance. From this we will attempt to compute the energy dissipated when a capacitor is immersed in the medium.

Starting with Maxwell's equations and the following definitions,

$$\text{curl } H - \frac{\partial D}{\partial t} - J = 0 , \quad (27)$$

$$\text{curl } \mathbf{E} + \frac{\partial \mathbf{B}}{\partial t} = 0, \quad (28)$$

$$D_i = \epsilon'_{ij} E_j, \quad (29a)$$

$$J_i = \sigma'_{ij} E_j, \quad (29b)$$

$$H_i = \mu_{ij} B_j, \quad (29c)$$

we can obtain an expression for the effective value of ϵ .
Assuming that all quantities have the time dependence $e^{i\omega t}$, we can write for equation (27)

$$\text{curl } \mathbf{H} - \frac{\partial}{\partial t} (\mathbf{D} + \int \mathbf{J} dt) = 0,$$

$$\text{curl } \mathbf{H} - \frac{\partial}{\partial t} (\mathbf{D} + \frac{1}{i\omega} \mathbf{J}) = 0.$$

In component form, by using (28a) and (28b), (27) becomes

$$(\text{curl } \mathbf{H})_i = \frac{\partial}{\partial t} \left[(\epsilon'_{ij} + \frac{1}{i\omega} \sigma'_{ij}) E_j \right],$$

$$i, j = 1, 2, 3.$$

Define $D_{\text{effective}}$ as

$$(D_{\text{effective}})_i = (\epsilon'_{ij} + \frac{1}{i\omega} \sigma'_{ij}) E_j = f_{ij} E_j, \quad (30)$$

then

$$\text{curl } H = \frac{\partial D}{\partial t} \text{effective} \quad (31)$$

f_{ij} may now be associated with the matrix defined in equation (26). This association will enable the Poynting theorem to be applied to the field quantities. If we have a surface S in space containing a volume V , then the net energy W passing out through the surface can be computed.

$$W = - \int_V \text{div}(\mathbf{E} \times \mathbf{H}) \, dV,$$

or

$$W = \frac{1}{4} \int_V \left[(\mathbf{E} + \mathbf{E}^*) \cdot \frac{\partial}{\partial t} (\mathbf{D} + \mathbf{D}^*) + (\mathbf{H} + \mathbf{H}^*) \cdot \frac{\partial}{\partial t} (\mathbf{B} + \mathbf{B}^*) \right] \, dV,$$

where \mathbf{E}^* is the complex conjugate of \mathbf{E} . A time average over one cycle is

$$W_{\text{av}} = \frac{1}{4} \int_V \left[(\mathbf{E} \cdot \frac{\partial}{\partial t} \mathbf{D}^* + \mathbf{E}^* \cdot \frac{\partial}{\partial t} \mathbf{D} + \mathbf{H} \cdot \frac{\partial}{\partial t} \mathbf{B}^* + \mathbf{H}^* \cdot \frac{\partial}{\partial t} \mathbf{B}) \right] \, dV,$$

$$W_{av} = \frac{i\omega}{4} \int_V \left[(E_1^* f_{1j} E_j - E_1 f_{1j}^* E_j^* + H_1^* \mu_{1j} H_j - H_1 \mu_{1j}^* H_j^*) \right] dV .$$

If there are no magnetic losses, that is $\mu_{1j} = \mu_{1j}^*$, then W_{av} becomes

$$W_{av} = \frac{i\omega}{4} \int_V \left[(E_1^* f_{1j} E_j - E_1 f_{1j}^* E_j^*) \right] dV . \quad (32)$$

Equation (32) gives the rate of heat generation in a given volume of the medium due to electromagnetic sources. The quantities E_1 are just the amplitudes of the electric field because of the time averaging. Performing the operations indicated in equation (32) we have

$$W_{av} = \int_V \frac{i\omega}{4} \left[|E|^2 (K_T - K_T^*) + |E|^2 \cos^2(E, H) (K_P - K_P^* + K_T - K_T^*) + i(K_H - K_H^*) (E_2^* E_1 - E_1^* E_2) \right] dV , \quad (33)$$

where (E, H) represents the angle between E and H , and

$$|E|^2 = |E_1|^2 + |E_2|^2 + |E_3|^2 ,$$

$$K_T^* - K_T = \frac{2iXZ(Z^2 + Y^2 + 1)}{(Y^2 + Z^2 - 1)^2 + 4Z^2} ,$$

$$K_P^* - K_P = \frac{2iXZ}{1 + Z^2} ,$$

$$K_H^* - K_H = \frac{4kxz}{(y^2 + z^2 - 1)^2 + 4kz^2}.$$

Thus, W_{av} is a real quantity and it is greater than zero. Assume that the inhomogeneity of the medium is such that K_T , K_P , and K_H vary slowly over the region strongly influenced by the capacitor. In the ionosphere, with a capacitor whose largest linear dimension is on the order of one meter, the assumption is excellent.

$$W_{av} = \frac{i\omega}{4} (K_T - K_T^*) \int_V |E|^2 dV + \frac{i\omega}{4} (K_P - K_P^* + K_T^* - K_T^*) \cdot \int_V |E|^2 \cos^2(E, H) dV + \frac{i\omega}{4} (K_H - K_H^*) \int_V (E_2^* E_1 - E_1^* E_2) dV \quad (34)$$

The integrals that are contained in equation (33) reflect the influence of the geometry. Unfortunately, for many practical geometries closed form integration is impossible. This is certainly true for the conical rocket capacitor.

4.5 TWO DIMENSIONAL APPROXIMATION TO THE ELECTRIC FIELD

The amount of work necessary to obtain an accurate numerical integration of Laplace's equation for the split cylinder is too much in three dimensions. A reasonable approximation to the fields may be had by treating the corresponding two dimensional problem. It is well known that only a few two dimensional electro-

static problems may be rotated to yield a three dimensional solution to Laplace's equation, but even so the qualitative features of the field will be retained.

The fringing field produced by the cylindrical capacitor is of primary interest, because it is only this field which contributes to the heat dissipation in the surrounding medium. The field surrounding the cylinder, in the quasistatic case, may be found from

$$\nabla^2 v = 0 . \quad (35)$$

Equation (35) may be solved using the general Schwarz transformation. This transformation is governed by the differential equation,

$$\frac{ds_1}{ds_2} = C \prod_{i=1}^n (s_2 - a_i)^{(b_i - \pi)/\pi}$$

n = one less than the number of vertices in the polygon forming the boundary.

C = a constant, possibly complex, which specifies the orientation of the polygon with respect to a set of axes in the s_1 plane.

a_i = the location of the i th vertex in the s_2 plane.

b_1 = the interior vertex angle measured in a counterclockwise sense.

The boundaries in the z plane are first transformed into the u axis of the t plane, and then to the w plane where the stream function s and the potential function V form a rectangular coordinate system. The Schwarz transformation for this case is

$$\frac{dz}{dt} = C \frac{\sqrt{t-1}}{t}.$$

Integrating, we obtain

$$z = C (\sqrt{t-1} - \tan^{-1}\sqrt{t-1}) + C', \quad (36)$$

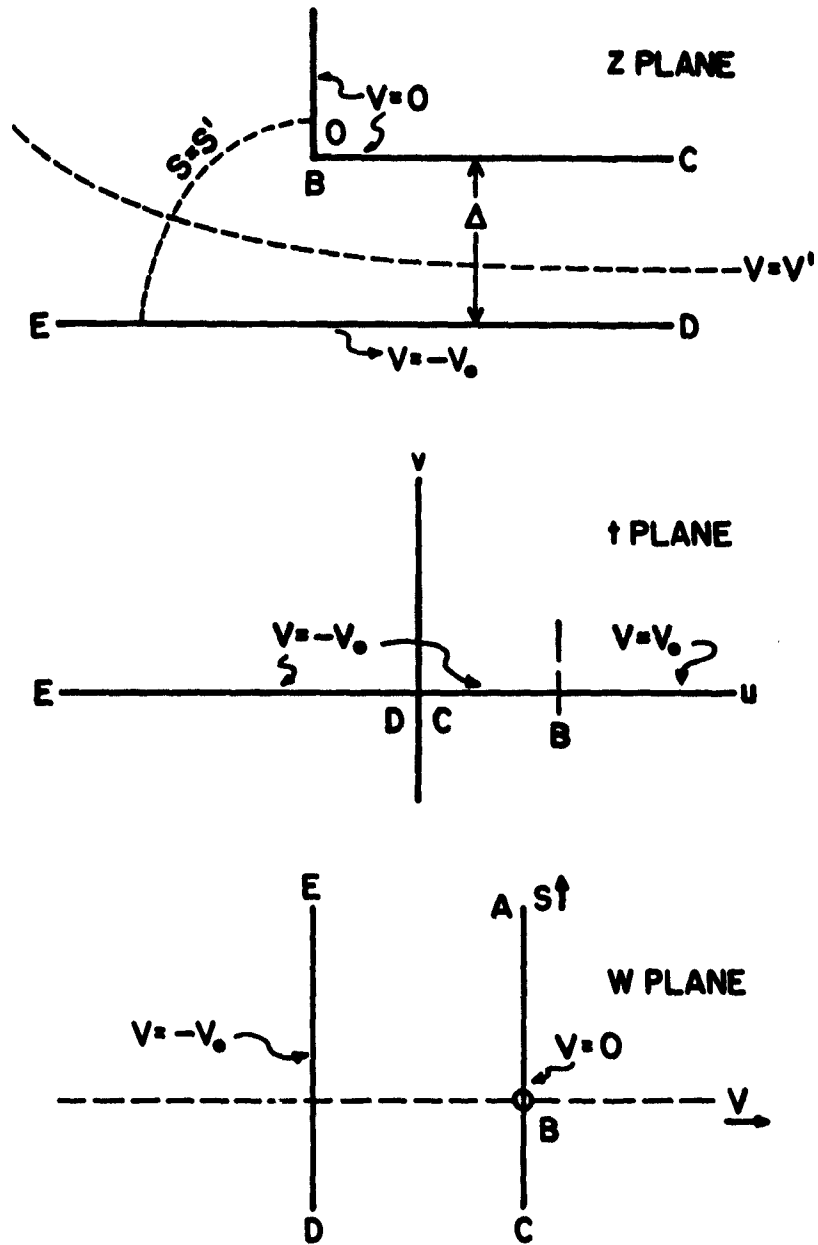
where C' may be set to zero.

Assume that we are in the region where $t < 0$, then $t - 1 < 0$. Set $\sqrt{t-1} = im$, where m is positive, then

$$\begin{aligned} \tan^{-1}\sqrt{t-1} &= \frac{1}{2} \ln \frac{1+m}{1-m} \\ &= \frac{\pi}{2} - \frac{1}{2} \ln \frac{m-1}{m+1}. \end{aligned}$$

When $z = i\Delta$, $m = 1$ and

$$C = \frac{2i\Delta}{\pi}.$$



THE Z, t, AND W TRANSFORMATION PLANES

FIGURE 5

Then equation (36) becomes

$$s = \frac{2i\Delta}{\pi} (\sqrt{t-1} - \tan^{-1}\sqrt{t-1}) . \quad (37)$$

Equation (37) maps the upper half of the s plane into the upper half of the t plane, and places the point B at $t = 1$.

In order to map the t plane into the w plane, the transformation is easily seen to be

$$t = e^{-i\pi\omega/V_0} . \quad (38)$$

To verify the transformation, let $t = |m|$. Then

$$V_0 \ln |m| = -i\pi V + \pi s ,$$

$$s = \frac{V_0}{\pi} \ln |m| ,$$

$$V = 0 .$$

When $t = -|m|$, then

$$V_0 \ln(-|m|) = -i\pi V - \pi s ,$$

$$V = -V_0 ,$$

$$s = \frac{V_0}{\pi} \ln |m| .$$

Therefore, the boundaries are mapped as required. The first transformation may be similarly verified. The potential V ranges from $-V_0$ to 0, and the stream function s from $-\infty$ to $+\infty$.

For the transformation to be useful, we combine the two equations (37) and (38) and write the total transformation in real and imaginary parts.

$$z = x + iy = \frac{2\Delta}{\pi} \left(\frac{1}{2} \ln \frac{r}{R} - b_1 \right) + i \frac{2\Delta}{\pi} \left(a_1 + \frac{g}{2} - \frac{d}{2} \right), \quad (39)$$

where the quantities r , R , b_1 , a_1 , g , and d are related to V and s by the following set of definitions:

$$a_1 = \left[(e - 1)^2 + f^2 \right]^{\frac{1}{4}} \left(\cos \left(\frac{1}{2} \tan^{-1} \frac{f}{e - 1} \right) \right), \quad (40a)$$

$$b_1 = \left[(e - 1)^2 + f^2 \right]^{\frac{1}{4}} \left(\sin \left(\frac{1}{2} \tan^{-1} \frac{f}{e - 1} \right) \right), \quad (40b)$$

$$e = \exp \left(\pi \frac{s}{V_0} \right) \cos \left(\pi \frac{V}{V_0} \right), \quad (40c)$$

$$f = -\exp \left(\pi \frac{s}{V_0} \right) \sin \left(\pi \frac{V}{V_0} \right), \quad (40d)$$

$$r = \sqrt{(1 + b)^2 + a^2}, \quad (40e)$$

$$g = \tan^{-1} \frac{a}{1+b}, \quad (40f)$$

$$R = \sqrt{(1-b)^2 + a^2}, \quad (40g)$$

$$d = \tan^{-1} \frac{a}{1-b}. \quad (40h)$$

Values of V and s are now inserted into the above set of equations. Connecting points of equal V , and similarly for equal s , constitutes a two dimensional mapping of the potential and the stream functions. The electric field vector is everywhere tangent to the stream function. The components of the electric field may be calculated from the total Schwarz transformation.

$$z = \frac{21\Delta}{\pi} \left[(e^{-i\pi\frac{w}{V_0}} - 1)^{\frac{1}{2}} - \tan^{-1}(e^{-i\pi\frac{w}{V_0}} - 1)^{\frac{1}{2}} \right],$$

$$E_x = \operatorname{Re} \left(-\frac{dw}{dz} \right),$$

and

$$E_y = \operatorname{Im} \left(-\frac{dw}{dz} \right).$$

Taking the derivative $\frac{dw}{dz}$ is lengthy, but easy. The final result is

$$-\frac{dw}{ds} = \frac{V_0/2\Delta}{G^2 + F^2} (G - iF).$$

Therefore,

$$E_x = -\frac{V_0}{2\Delta} \frac{G}{G^2 + F^2}, \quad (41)$$

$$E_y = \frac{V_0}{2\Delta} \frac{F}{G^2 + F^2}, \quad (42)$$

where

$$G = -2 \left[1 - \left(\frac{e^{-\pi \frac{s}{V_0}}}{2\sqrt{R_1}} \right) \left(\cos \pi \frac{V}{V_0} \cos \frac{P}{2} - \sin \pi \frac{V}{V_0} \sin \frac{P}{2} \right) \right],$$

$$F = -2 \left[\frac{e^{-\pi \frac{s}{V_0}}}{2\sqrt{R_1}} \right] \left[-\sin \pi \frac{V}{V_0} \cos \frac{P}{2} - \cos \pi \frac{V}{V_0} \sin \frac{P}{2} \right],$$

$$R_1 = \left[\cos^2 \left(\pi \frac{V}{V_0} \right) \exp \left(\pi \frac{s}{V_0} \right) + \sin^2 \left(\pi \frac{V}{V_0} \right) \right]^{\frac{1}{2}},$$

$$P = \tan^{-1} \left[\frac{-\sin \pi \frac{V}{V_0}}{\cos \left(\pi \frac{V}{V_0} \right) \exp \left(\pi \frac{s}{V_0} \right)} \right].$$

Equations (41) and (42) determine the quantity $|E|^2$ in

equation (33).

The angle between the electric and magnetic fields must now be calculated at each point in space. A coordinate system with one axis tangent to the earth at the point of the rocket launching and another perpendicular to the earth makes a convenient reference system. Measuring all angles from the horizontal axis yields

$$(E,H) = \frac{\pi}{2} + L - \tan^{-1} (E_y / E_x) - H'.$$

H' = the angle that the magnetic field makes with the horizontal in radians.

L = the launch angle in radians

It is now possible to perform the integration in equation (33) numerically. However, one further simplification is in order. Suppose there exists a conformal mapping, such as a Schwarz transformation, between the z plane and the w plane.

Consider the integral

$$\iint_{S'} \cos^2 (E,H) dV ds,$$

and

$$dV = \frac{\partial V}{\partial x} dx + \frac{\partial V}{\partial y} dy,$$

$$ds = \frac{\partial s}{\partial x} dx + \frac{\partial s}{\partial y} dy ,$$

where $s = x + iy$ and $w = V + is$.

Squaring and adding,

$$(dV)^2 + (ds)^2 = \left[\left(\frac{\partial V}{\partial x} \right)^2 + \left(\frac{\partial V}{\partial y} \right)^2 \right] \left[(dx)^2 + (dy)^2 \right] ,$$

where the Cauchy Reimann equations,

$$\frac{\partial V}{\partial x} = \frac{\partial s}{\partial y}$$

and

$$\frac{\partial V}{\partial y} = - \frac{\partial s}{\partial x} ,$$

have been used. Therefore,

$$(dV)^2 + (ds)^2 = |E|^2 \left[(dx)^2 + (dy)^2 \right] .$$

This determines the differential element in the transformed plane. Thus, $dV ds$ becomes $|E|^2 dx dy$, and

$$\iint_{\mathfrak{B}'} \cos^2(E,H) dV ds = \iint_{\mathfrak{B}} |E|^2 \cos^2(E,H) dx dy . \quad (43)$$

Since the mapping is conformal, (E, H) transforms unchanged.

Equation (43) reduces the difficulty of performing the integration. The limits of integration are now more difficult to determine in the untransformed space. The object is to select a region of space sufficiently large so that almost all of the power is dissipated within the chosen volume. If the limits are selected in the transformed space, and then carried over to the untransformed space, an appropriate boundary may be determined. The most convenient boundary lies along one of the lines of constant stream function.

The integration and computation was performed on an I.B.M. 7074 computer. The results of this computation are displayed in the next section. An interesting feature of the computation was that the last term of equation (33) turned out to be quite small compared with the rest of the terms. This term can be rearranged to resemble a polarisation term in the magnetoionic theory by some algebraic manipulation. Essentially, it is a measure of the anisotropy of the polarizability of the medium. Thus, for the region below 150 km this anisotropy is a negligibly small effect. This result is just what is expected on the basis of qualitative argument.

When the magnetic field H and the electric field E are specified, equation (33) can be written

$$W_{av} = \frac{V_0^2}{\Delta^2} f(N, \nu, \omega) .$$

The total power dissipated by the fields from the cylindrical capacitor is approximately $2\pi W_{av} = Q$, or

$$Q = 2\pi \frac{V_0^2}{\Delta^2} f(N, \nu, \omega) = \frac{V_0^2}{2R} , \text{ (in joules/second)}$$

where V_0 is the peak voltage and R the effective resistance. Then it follows that

$$R = \frac{\Delta^2}{4\pi f(N, \nu, \omega)} \quad \text{(in ohms)} . \quad (44)$$

Equation (44) determines the effective resistance of the medium in which the capacitor is immersed. No information results from this method about the capacitive portion of the impedance.

It is obvious that the procedure just outlined is far from an ideal treatment of the problem. The greatest difficulty being that the answers obtained are extremely sensitive to the method used in evaluating the effects of the electric field near the cylinder. The two dimensional field solution yields only the grosser features of the electric field surrounding the capacitor, since the cylindrical rotation of this field does not represent

the true three dimensional electric field. The information that it does contain, namely the qualitative behavior of the losses due to heat dissipation, is useful.

4.6 APPLICATION OF THE DEFINITION OF CAPACITANCE

A better approach, for the computation of the impedance characteristics of the capacitor, is to return to the basic definition of capacitance in any medium. In a strict operational sense this definition is

$$C = \frac{q}{V} ,$$

where q = the charge on the plates of the capacitor in coulombs, and V = the potential difference between the plates in volts. The definition can be written in a more useful form by expressing q and V in terms of integrals of the field quantities.

$$C = \frac{\int D \cdot \underline{n} \, dS}{\int E \cdot d\underline{L}} , \quad (45)$$

where \underline{n} = the unit normal to the surface of the capacitor,
 dS = a surface element on the capacitor plates,
 and \underline{L} = a path along which E is integrated between the plates.

Equation (45) becomes

$$C = \frac{1}{V} \int_S \underline{D} \cdot \underline{n} \, dS \quad .$$

However, $\underline{n} = \frac{\underline{E}_s}{|\underline{E}_s|}$, where \underline{E}_s is the electric field at the surface of the capacitor. Then

$$C = \frac{1}{V} \int \frac{\underline{D} \cdot \underline{E}_s}{|\underline{E}_s|} \, dS \quad , \quad (46)$$

$$C = \frac{1}{V} \int \frac{E_i \epsilon_{ij} E_j}{|\underline{E}_s|} \, dS \quad . \quad (47)$$

By an analysis similar to that for equation (33), we have

$$C = \frac{1}{V} \int |\underline{E}_s| \left[K_T + (K_P - K_T) \cos^2(\underline{E}, \underline{H}) \right] \, dS \quad . \quad (48)$$

The definitions of the quantities K_T and K_P are the same as in equation (33).

If the same capacitor is evaluated in free space, then its capacitance will be

$$C_0 = \frac{1}{V} \int_S \epsilon_0 |\underline{E}| \, dS \quad . \quad (49)$$

Since neither K_P nor K_T varies over the dimensions of the rocket,

$$\frac{C}{C_0} = \frac{K_T}{\epsilon_0} + \frac{K_P - K_T}{\epsilon_0} \frac{\int |\underline{E}| \cos^2(\underline{E}, \underline{H}) \, dS}{\int |\underline{E}| \, dS} \quad . \quad (50)$$

If the nose of the rocket is slender, that is, if its apex angle is small, then by using the angular symmetry of the rocket, equation (50) becomes

$$\frac{C}{C_0} = \frac{K_T}{\epsilon_0} + \frac{K_P - K_T}{\epsilon_0} \langle \cos^2(\mathbf{E}, \mathbf{H}) \rangle, \quad (51)$$

where

$$\langle \cos^2(\mathbf{E}, \mathbf{H}) \rangle = \frac{2}{2\pi} \int_{|\langle \mathbf{E}, \mathbf{H} \rangle_{\min}|}^{|\langle \mathbf{E}, \mathbf{H} \rangle_{\max}|} \cos^2(\mathbf{E}, \mathbf{H}) d(\mathbf{E}, \mathbf{H}) . \quad (52)$$

When the electron density is vanishingly small, and the collision frequency is very high, K_T and K_P approach ϵ_0 , or C/C_0 approaches 1.

The first term in equation (51) displays the isotropic portion of the capacitor's characteristics, while the second term gives the orientation sensitive behavior. The quantity $\langle \cos^2(\mathbf{E}, \mathbf{H}) \rangle$ is readily determined from a knowledge of the launch angle and telemetered aspect data for every point during the rocket's flight. The earth's magnetic field is assumed to make a constant angle with some arbitrary fixed reference throughout the flight.

It is clear that the evaluation of equation (52) can easily be made for many different geometries in closed form. In addition, an evaluation of equation

(50) may be made on a digital computer with great accuracy and comparative ease. This is certainly not the case with equation (44).

4.7 EQUIVALENT CIRCUIT REPRESENTATION

If both the developments presented here are to be considered valid, then they must show the same qualitative behavior as a function of the ionospheric parameters. A numerical comparison of the two developments appears in the next section.

The quantities calculated must now be specifically identified. This will be done with the aid of a schematic circuit representation of the actual physical situation.

As was stated before, the capacitance and the conductance calculated in equations (20) and (21) relate to the fluctuations of the ion sheath surrounding the vehicle. This may be represented by a capacitor shunted by a resistor between the surface of the cylinder and the sheath edge for each half. The capacitance calculated in equation (51) is a complex number which contains both resistive and reactive terms. Writing C/C_0 in its real and imaginary parts, we have

$$C = C_0 (a + ib) ,$$

The quantities a and b are defined in terms of the real and imaginary parts of K_P and K_T (written $\text{Re}(K_P)$, $\text{Re}(K_T)$, $\text{Im}(K_P)$, and $\text{Im}(K_T)$).

$$\text{Re}(K_P) = \epsilon_0 - \frac{X}{1 + Z^2} \quad .$$

$$\text{Im}(K_P) = - \frac{ZX}{1 + Z^2} \quad .$$

$$\text{Re}(K_T) = \epsilon_0 + \frac{X(Y^2 - Z^2 - 1)}{(Y^2 + Z^2 - 1)^2 + 4Z^2} \quad .$$

$$\text{Im}(K_T) = - \frac{XZ(Y^2 + Z^2 + 1)}{(Y^2 + Z^2 - 1)^2 + 4Z^2} \quad .$$

Then for the impedance Z_1 of this complex element, we have

$$Z_1 = \frac{1}{i\omega C} \quad , \quad \omega = 2\pi f$$

$$Z_1 = \frac{-b}{\omega C_0 (a^2 + b^2)} + i \frac{-a}{\omega C_0 (a^2 + b^2)} \quad .$$

Identifying the real and imaginary parts as the series resistive R_s and reactive X_s parts respectively, yields

$$R_s = \frac{-b}{\omega C_0 (a^2 + b^2)} \quad ,$$

$$X_s = \frac{-a}{\omega C_0 (a^2 + b^2)} \quad .$$

R_s and X_s may be converted into their equivalent parallel

circuit components, R_p and X_p respectively, by

$$R_p = \frac{R_s^2 + X_s^2}{R_s} \quad , \quad (53)$$

$$X_p = \frac{R_s^2 + X_s^2}{X_s} \quad . \quad (54)$$

Noting that the conductance G in equation (21) is just the reciprocal of the resistance, we may now complete the identification of the resistive and reactive components. Labeling the capacitance derived in equation (20) as C_2 and the resistance from equation (21) as R_2 , the quantities R_p , X_p , R_2 , and C_2 may be combined into a single capacitor C_{PT} and a single resistor R_{PT} shunting the oscillator. The total impedance of the resulting circuit will be the value actually measured by an impedance bridge contained within the rocket. The reduction of the physical circuit to one which contains only one reactive element and one resistive element in parallel with it is quite standard.

Each half of the rocket capacitor interacts with the sheath to produce a capacitance C_2 and a resistance R_2 . These four components can be reduced to their series equivalents R_{2s} and X_{2s} .

$$R_{2s} = \frac{2R_2}{1 + \omega^2 C_2^2 R_2^2} \quad ,$$

$$X_{2s} = - \frac{2\omega C_2 R_2^2}{1 + \omega^2 C_2^2 R_2^2} .$$

Changing R_{2s} and X_{2s} into two parallel components R_{p2} and X_{p2} by

$$R_{p2} = \frac{R_{2s}^2 + X_{2s}^2}{R_{2s}} ,$$

and
$$X_{p2} = \frac{R_{2s}^2 + X_{2s}^2}{X_{2s}} .$$

Combining R_{p2} and X_{p2} with R_p and X_p we obtain the expressions for R_{pT} and X_{pT} . These are

$$R_{pT} = \frac{R_p R_{p2}}{R_p + R_{p2}} , \tag{55}$$

$$X_{pT} = \frac{X_p X_{p2}}{X_p + X_{p2}} . \tag{56}$$

Equations (55) and (56) are the relation between the measured impedance and the electron density.

5. NUMERICAL EVALUATION OF THE THEORETICAL RESULTS

Equations (44), (55), and (56) were numerically evaluated with the aid of an I. B. M. computer. The data for the electron density, temperature, and collision frequency were obtained from ionospheric models as incorporated into CIRA 1961. An experimental determination of the rocket's velocity made from similar rockets during test flights yielded the approximate result

$$v^2 = 3.35 \times 10^6 - 16.85 \times 10^3 h,$$

for altitudes greater than 40 km. The altitude h is in kilometers and the velocity v in meters per second. The rocket launch angle was taken at 85° with respect to the horizontal, and the angle (u, s) between the rocket axis and its velocity vector for every point of its trajectory is approximately given by

$$(u, s) = \tan^{-1} 10.5 - \tan^{-1} (-2.5 \times 10^{-4} d + 10.5),$$

where $d = 4.2 \times 10^4 (1 \pm \sqrt{0.88 - 4.6 \times 10^{-3} h})$.

The data for the magnetic field strength, 6.07×10^{-5} webers per square meter, and angle with respect to the horizontal, 58° , were used as approximate figures for what might be encountered at the launch site. The oscillator frequencies were taken to be 1.0×10^5 and 5.12×10^5 cycles per second to correspond to the planned rocket flight.

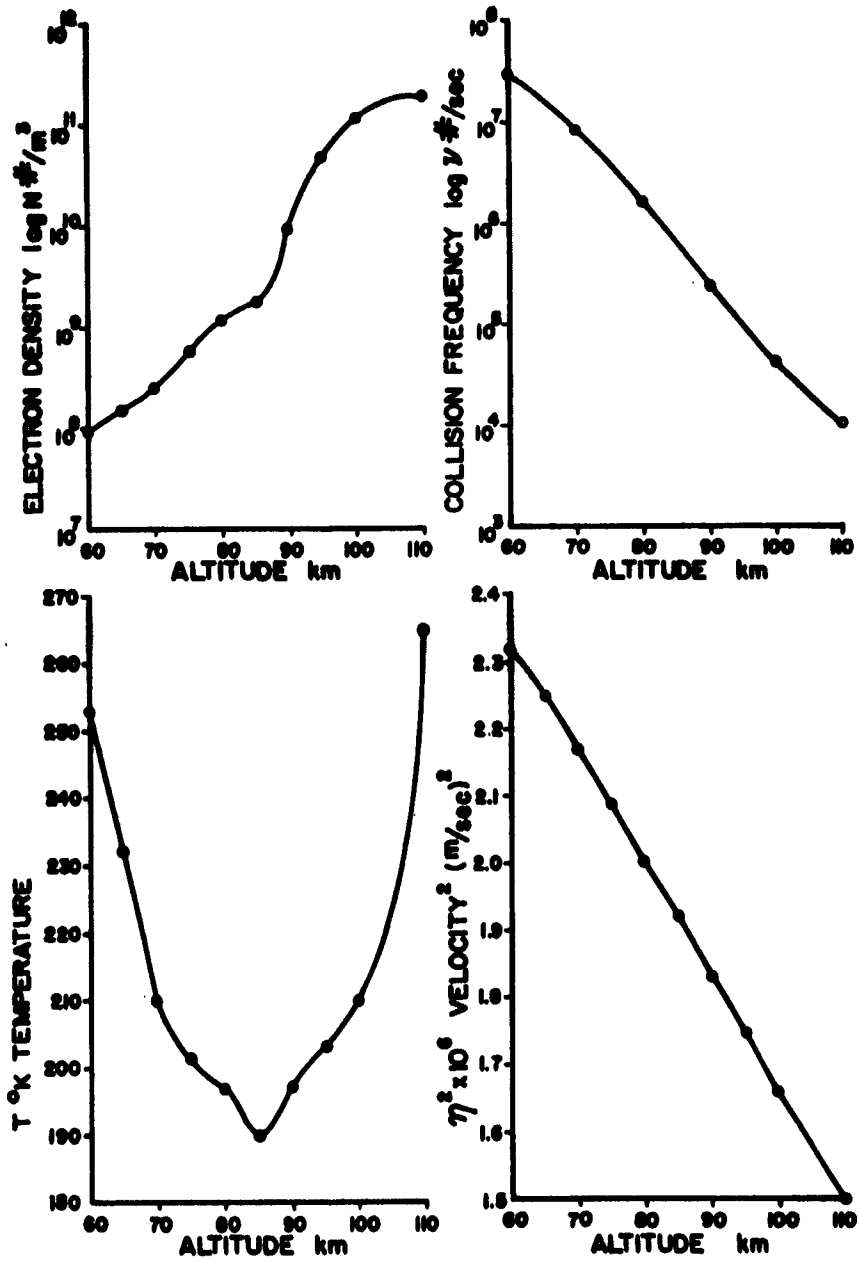
The results of these computations are shown in

the accompanying graphs. Figure 6 displays the ionospheric models used. Figure 7 shows the resistive component of the complex impedance as a function of altitude, and similarly Figure 8 for the reactive component. The values given in Figures 7 and 8 neglect the resistive and reactive contributions from the inside of the rocket. Thus, to actually interpret experimental results the data must be adjusted to account for the internal contributions. Since the interior of the rocket is sealed from the effects of the ionosphere, the adjustment to the data should be a constant throughout the flight.

Figure 9 is a plot of the resistive component obtained in equation (44) and the resistive component obtained from equation (53). Since these are supposed to represent the same circuit element, at least qualitatively, they have been plotted together for purposes of comparison.

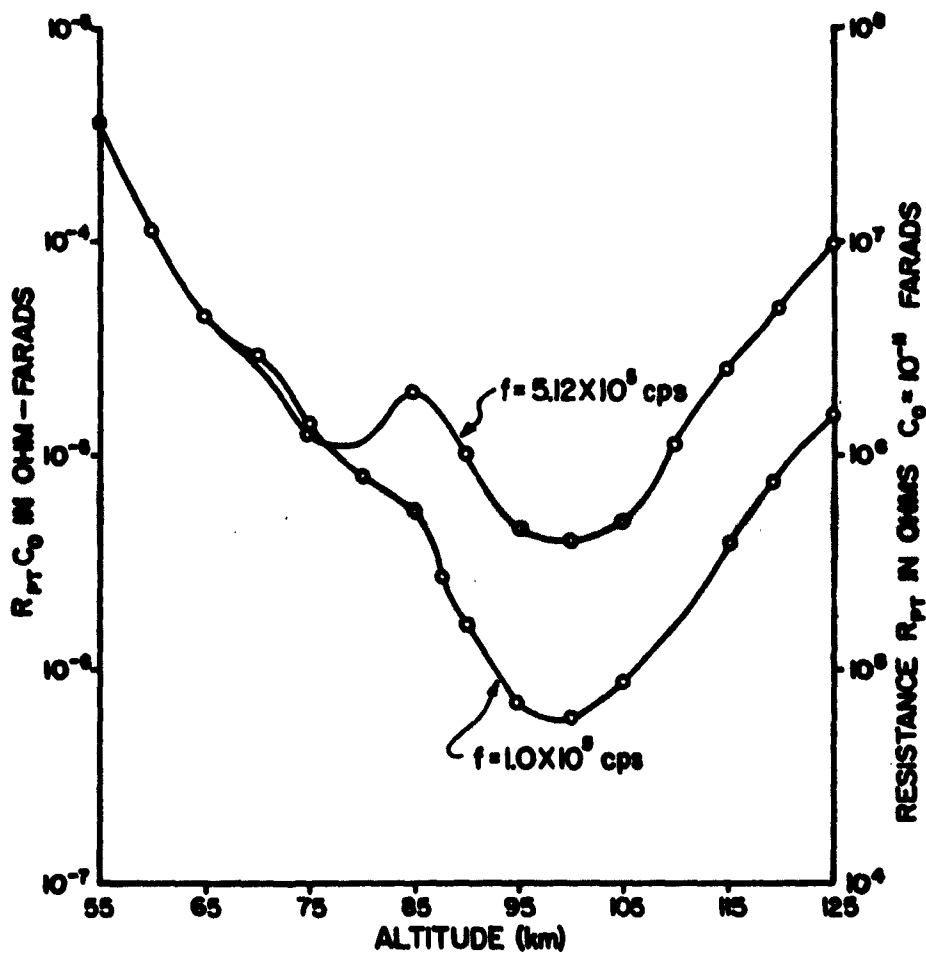
The left hand ordinates of Figure 7 to Figure 11 are multiplied by the capacitance C_0 measured in free space, while the right hand ordinates give the resistance and reactance for $C_0 = 1.0 \times 10^{-11}$ farads. The value of C_0 selected is representative for this type of experiment.

The application of magnetoionic theory alone, as developed in section 4.4, leads to probe impedance curves whose general form is not altered over a wide range of oscillator frequencies below 2 mc. The frequency 2 mc



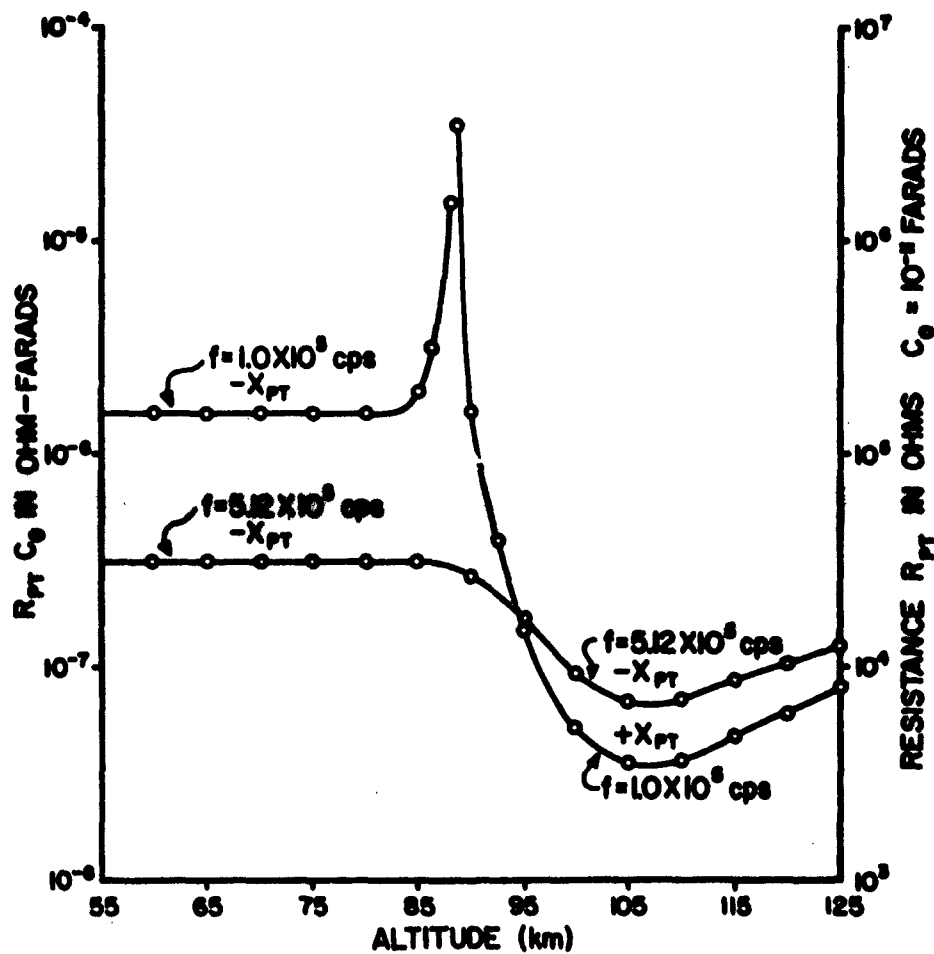
IONOSPHERIC MODEL FOR THE ROCKET PROBE

FIGURE 6



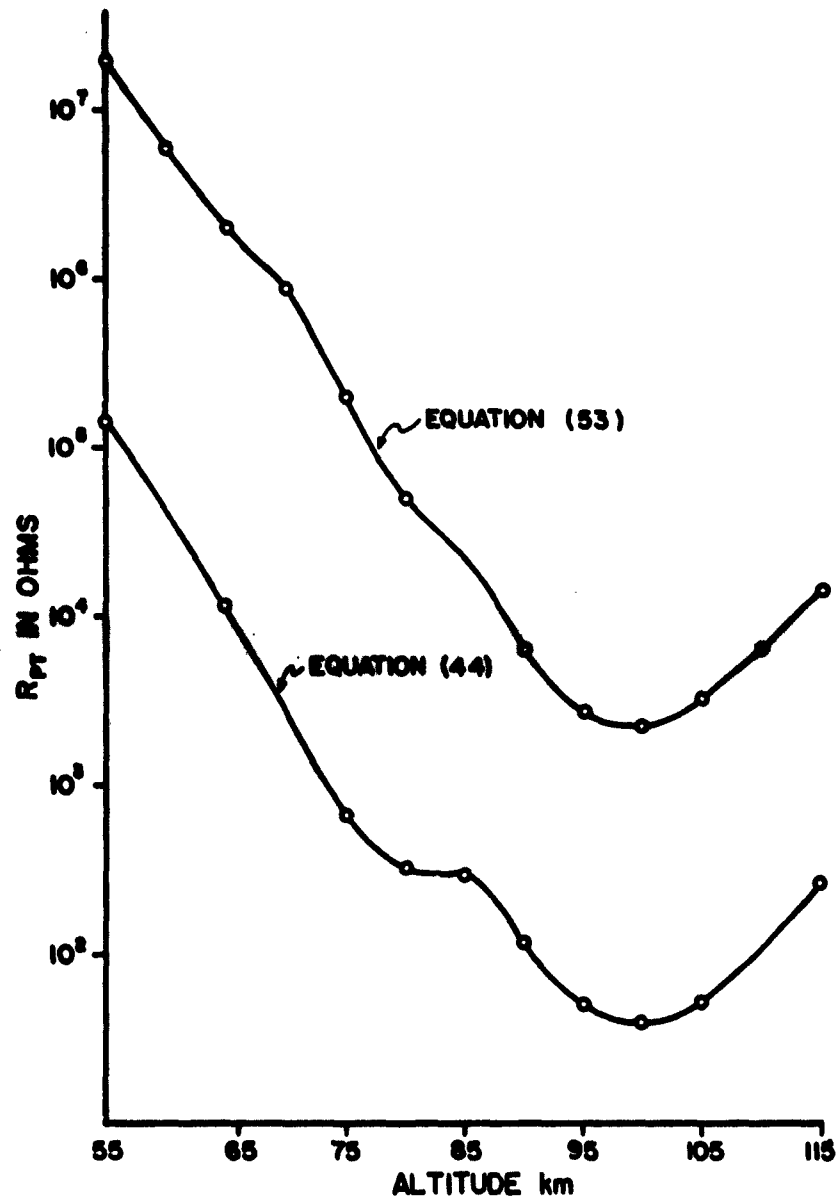
TOTAL PARALLEL RESISTANCE R_{PT} FOR TWO OSCILLATOR FREQUENCIES

FIGURE 7



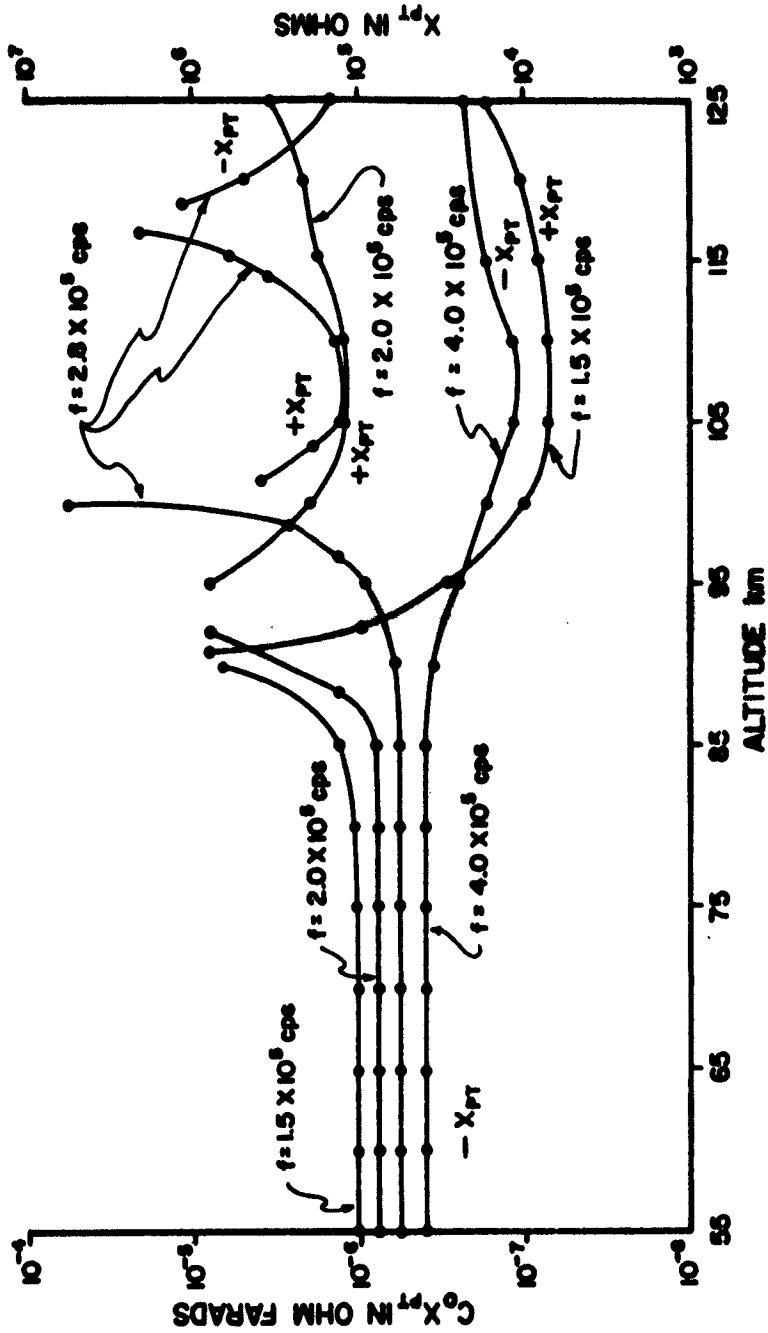
TOTAL PARALLEL REACTANCE X_{PT} FOR TWO OSCILLATOR FREQUENCIES

FIGURE 8



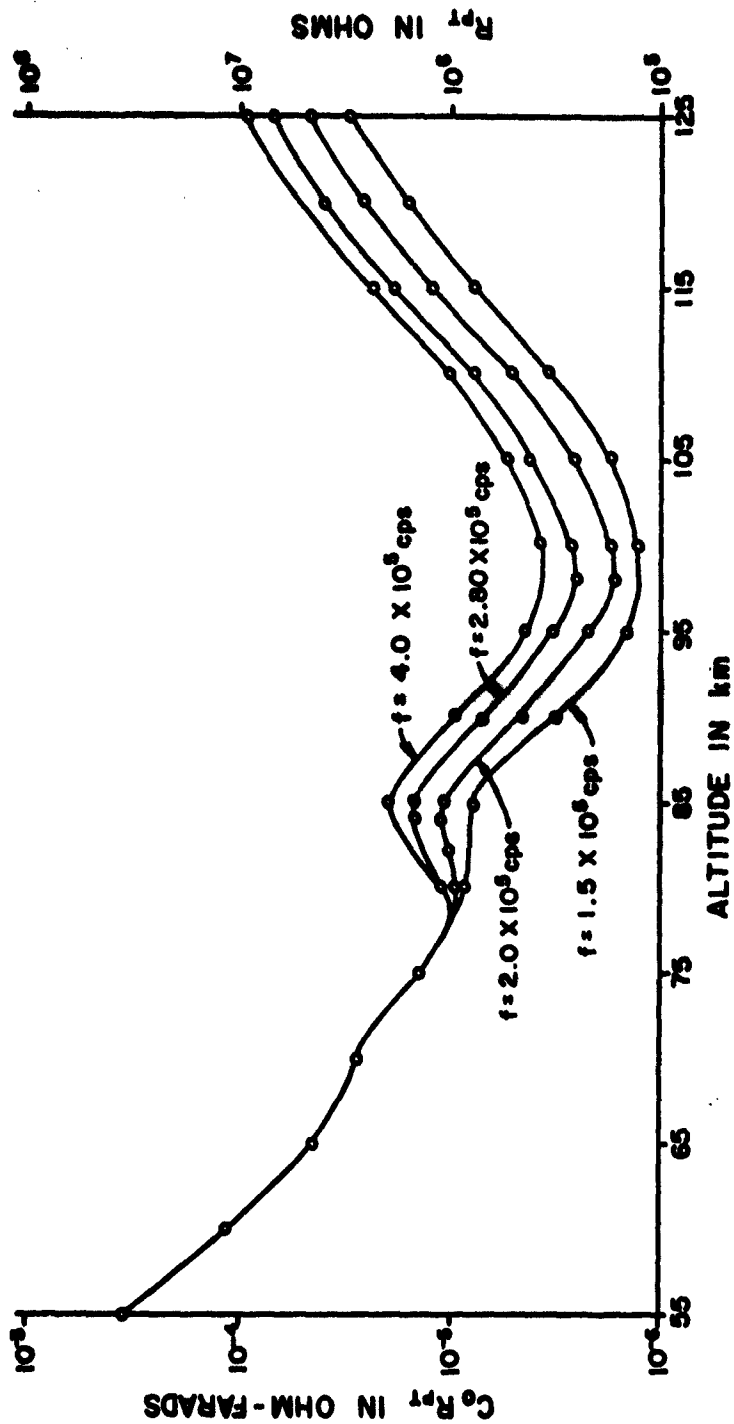
A PLOT OF R_{PT} VS ALTITUDE SHOWING SIMILAR QUALITATIVE BEHAVIOR FOR THE TWO METHODS OF COMPUTING R_{PT}

FIGURE 9



TOTAL PARALLEL REACTANCE FOR FOUR OSCILLATOR FREQUENCIES

FIGURE 10



TOTAL PARALLEL RESISTANCE FOR FOUR OSCILLATOR FREQUENCIES

FIGURE 11

was an arbitrary computational limit. The general form of the reactance curves for the above frequency range is that shown in Figure 8 for $f = 1.0 \times 10^5$ cps. The resistance curves follow the form of the curves in Figure 7. The smooth transition between curves of different frequencies is the notable result for the magnetoionic calculation.

The addition of the effects of the ion and electron currents flowing to the rocket from the ionosphere, developed in sections 4.0 to 4.3, alters the impedance characteristics considerably. Now the shape of the reactance curves shows a marked frequency dependence. At frequencies less than 2.5×10^5 cps the reactance undergoes a change from negative capacitive values to positive inductive values in the vicinity of 100 km. This change moves towards higher altitudes as the frequency increases. For the frequency range 2.5×10^5 cps to 2.95×10^5 cps, a second change back to negative reactance occurs. Above 2.95×10^5 cps there are no sign changes in the reactance until 2 mc where the reactance undergoes two sign changes again. The computations were carried out in the range 55 km to 130 km because above 130 km there is a lack of meaningful collision frequency and temperature data. The curves showing this frequency dependence are in Figure 10. Four representative curves showing the corresponding resistive component are in

Figure 11.

These results show the strong effect of the sheath on the impedance characteristics. In the lower portion of the altitude range considered, the contributions of the sheath are only a small portion of the total impedance. However, at altitudes higher than approximately 90 km the sheath effect contribute quite strongly. The second change in sign of the reactance is directly attributable to the sheath. Thus, neglecting the sheath contribution or the magnetoionic contribution would lead to serious error in the altitude range considered.

The theory developed will allow data for the measured value of the probe impedance to be reduced to electron density as a function of altitude. This is most easily done by computing an entire family of impedance characteristic curves and then obtaining the best fit to the raw data by inspection, or by the use of a suitable numerical smoothing technique.

6. CONCLUSION

A relationship between the measured impedance of a low frequency RF rocket probe, immersed in the ionosphere, and the electron density has been developed. This relationship will enable data, telemetered from the rocket to the ground, to be reduced into an electron density profile for the altitude range of 55 km to 130 km.

The problem was separated into two main sections. First, the formation of an ion sheath about the rocket probe was investigated so as to be able to determine its effects on the impedance of the probe. The main features of the sheath were determined by calculating the ion and electron currents from the ionosphere to the rocket probe, and requiring that they be equal at equilibrium. In order to apply the results, the oscillator frequency must be low enough so that is able to respond fully to the voltage changes. Second, a magnetoionic description of the ionosphere was developed to determine an effective dielectric constant to be applied to the capacitor. This description accounted for the oscillations of the electrons between the two halves of the capacitor. Since collisions were included in the description, a resistive and reactive contribution was found to result from the electron oscillations.

A schematic description of the electrical

properties of the ionosphere, as seen by an impedance bridge carried by the rocket, was developed. A single resistive and reactive element, each in parallel with the oscillator, was derived from the detailed schematic circuit. It is through these two elements that the contributions of the sheath and the electron oscillations were combined. The final result constitutes a relationship between the measured impedance and the electron density.

A model ionosphere was described and used to determine a set of resistance and reactance curves for a theoretical model of the rocket probe. These curves clearly indicate that the sheath effects and the magnetoionic effects were both important throughout the altitude range of interest. Above approximately 90 km, the contributions of the sheath to the total reactance actually dominate to produce a double change in sign for certain frequencies, and no change in sign for other frequencies. Alone, magnetoionic theory produces only a single change in sign in the reactance as a function of altitude.

There are obviously some drawbacks to this type of experiment. In order to calculate the impedance characteristics, it was assumed that a detailed model of the collision frequency, temperature, and ion mass is known accurately as a function of altitude. In general,

this is not the case. Therefore, such data must be obtained from a suitable experiment flown simultaneously with the capacitor rocket probe, or from theoretical models of the ionosphere.

6.1 SUGGESTIONS FOR FURTHER RESEARCH

Some refinements in the theory suggest themselves immediately. The sheath model should be obtained from a solution of Poisson's equation in which the charge distribution is a derived function rather than a specified one. The Maxwellian velocity distribution should be modified to account for both the presence of a solid boundary, and for the possibility of two different temperatures for ions and electrons. Fortunately, the temperature always enters in an insensitive way, so that errors introduced by an imprecise knowledge of the temperature at the time of the flight should be small. Finally, the cylinder used is an extreme idealization of the conical rocket. This might be improved upon by employing a split prolate spheroid instead.

Acknowledgment

The author wishes to express his appreciation to Dr. J. S. Wisbet, Dr. J. R. Mentzer, and Dr. J. J. Gibbons whose assistance made this work possible. The work of Mrs. Peggy Royer in performing the more difficult computations was of great assistance.

Johnson, E. O., and Malter, L., A Floating Double Probe Method for Measurements in Gas Discharges, Phys. Rev., 80, 58 (1950)

Kane, J. A., Jackson, J. E., and Whale, H. A., RF Impedance Probe Measurements of Ionospheric Electron Densities, J. Research NBS 66D, 641 (1962).

Langmuir, I., and Compton, K. T., Electrical Discharges in Gases, Rev. Mod. Phys., 3, 191 (1931).

Mlodnosky, R. F., and Garriott, O. K., The VLF Admittance of a Dipole in the Lower Ionosphere, International Conference on the Ionosphere, London, July 5, 1962.

Seddon, J. C., Propagation Measurements in the Ionosphere with the Aid of Rockets, J. Geophys. Research, 58, 323 (1953).

Smith, L. G., Rocket Measurements of Electron Density and Temperature in the Nighttime Ionosphere, AGU First Western National Meeting, Los Angeles, Dec. 27-29, 1961.

Stratton, J. A., Electromagnetic Theory, McGraw-Hill Book Co., New York (1941).

6. BIBLIOGRAPHY

Bourdeau, R. E., Whipple, E. C., and Clark, J. F., Analytic and Experimental Electrical Conductivity between the Stratosphere and the Ionosphere, J. Geophys. Research, 64, 1363 (1959).

Budden, K. G., Radio Waves in the Ionosphere, Cambridge University Press (1961).

Hoegy, W. R., and Brace, L. H., The Dumbbell Electrostatic Probe: Theoretical Aspects, Univ. of Mich. Res. Inst. Report JS-1 (1961)

Hok, G., Dynamic Probe Measurements in the Ionosphere, Univ. of Mich. Eng. Res. Inst. Report, 2521-5-s (1951).

Jackson, J. E., and Pickar, A. D., Performance of a Rocket Borne 7.75 Mc. Transmitting Antenna in the Ionosphere, Upper Atmosphere Rept. 28, U.S. Naval Research Laboratory Rept. 4940 (1957).

Jastrow, R., and Pearse, C. A., Atmospheric Drag on the Satellite, J. Geophys. Research, 62, 413 (1957).

Jahnke, E. and Emde, F., Tables of Functions, Dover (1938).